THE ASTROPHYSICAL JOURNAL, 471:68–81, 1996 November 1
© 1996. The American Astronomical Society. All rights reserved. Printed in U.S.A.

THE ANALYTICAL DISTRIBUTION FUNCTION OF ANISOTROPIC TWO-COMPONENT HERNQUIST MODELS

L. CIOTTI
Osservatorio Astronomico di Bologna, via Zamboni 33, I-40126 Bologna, Italy
Received 1996 March 25; accepted 1996 May 28

ABSTRACT

The analytical phase-space distribution function (DF) of spherical self-consistent galaxy (or cluster) models, embedded in a dark matter halo, where both density distributions follow the Hernquist profile, with different total masses and core radii (hereafter "HH models"), is presented. The concentration and the amount of the stellar and dark matter distributions are described by four parameters: the mass and core radius of the *reference* component and two dimensionless parameters that describe the mass and core radius of the *halo* component. A variable amount of orbital anisotropy is allowed in both components, following the widely used Osipkov-Merritt parameterization. An important case is obtained for a null core radius of the halo, corresponding to the presence of a central black hole (BH).

Before giving the explicit form for the DF, the necessary and sufficient conditions that the model parameters must satisfy in order to correspond to a *consistent* system (i.e., a system for which each physically distinct component has a positive DF) are analytically derived. In this context, it is proved that globally isotropic HH models are consistent for any mass ratio and core radii ratio, even in the case of a central BH. In this last case, the analytical expression for a lower limit of the anisotropy radius of the host system as a function of the BH mass is given. These results are then compared with those obtained by direct inspection of the DF. In the particular case of global isotropy, the stability of HH models is proved, and the explicit formula for the differential energy distribution is derived. Finally, the stability of radially anisotropic HH models is briefly discussed.

The expression derived for the DF is useful for understanding the relations between anisotropy, density shape, and external potential well in a consistent stellar system and to produce initial conditions for N-body simulations of two-component galaxies or galaxy clusters.

Subject headings: celestial mechanics, stellar dynamics — dark matter — galaxies: elliptical and lenticular, cD — galaxies: kinematics and dynamics — galaxies: structure

1. INTRODUCTION

Recent ground-based observations (Møller, Stiavelli, & Zeilinger 1995) and observations with the *Hubble Space Telescope* have shown that the spatial luminosity distributions of elliptical galaxies approach a power-law form $\rho(r) \propto r^{-\gamma}$ at small radii, with $0 \leq \gamma \leq 2.5$ (Crane et al. 1993; Jaffe et al. 1994; Ferrarese et al. 1994; Lauer et al. 1995; Kormendy et al. 1996; Byun et al. 1996). These findings increase considerably the interest of theorists in the study of cuspy models. Two important families of spherical dynamical models with a central divergent density that have been explored so far are the $R^{1/m}$ models and the so-called γ-models. The dynamical properties of models whose surface brightness distribution follows the $R^{1/m}$ law, introduced by Sersic (1968) as a natural generalization of the de Vaucouleurs (1948) law, have been extensively studied (Ciotti 1991; Ciotti & Lanzoni 1996). Particularly, their deprojected density increases toward the center as $r^{-(m-1)/m}$ for $m > 1$; unfortunately, two major problems afflict these models: their deprojected density cannot be expressed analytically in terms of known functions, and no galaxies with $\gamma > 1$ can be accurately modeled in their central regions. The family of the γ-models, in some way anticipated by Hernquist (1990, hereafter H90), has been widely explored (Dehnen 1993; Carollo 1993; Tremaine et al. 1994), and it represents a generalization of the well-known Hernquist (H90) and Jaffe (1983) density distributions. As shown by the previous authors, many of the dynamical properties of the γ-models can be expressed analytically. In particular, the Hernquist model (hereafter "H model") in projection well resembles the de Vaucouleurs law, and an exhaustive analytical investigation of its properties is possible (H90).

It is now accepted that a fraction of the mass in galaxies and clusters of galaxies is made of a dark component whose density distribution differs from that of the visible one. The shape of the dark matter distribution is not well constrained by observations, but numerical simulations of dissipationless collapse seem to favor a peaked profile, consistent with the scale-free nature of the gravitational field (Dubinski & Carlberg 1991; White 1996, and references therein). From these considerations it follows that the obvious generalization of the one-component spherical models (the dynamicist's zeroth-order approximation of real galaxies) is not only in the direction of the actively developed modeling of axisymmetric and triaxial systems (see, e.g., de Zeeuw 1996 for a recent review) but also in the study and construction of two-component analytical models, a field far less developed. From this point of view the zeroth-order approximation of realistic galaxies is the construction of analytical, spherically symmetric, *two-component* galaxy models.

When studying a dynamical model (single or multicomponent), the fact that the Jeans equations have a physically acceptable solution is not a sufficient criterion for the validity of the model: the essential requirement to be met by any acceptable dynamical model is the positivity of the distribution function (DF) of each physically distinct component. A model that satisfies this minimal requirement

© American Astronomical Society • Provided by the NASA Astrophysics Data System

(much weaker than the model stability) is called a *consistent* model. Two general strategies can be used to construct a consistent model or to check whether a proposed model is consistent: the "f to ρ" and the "ρ to f" approaches (Binney & Tremaine 1987, hereafter BT87). An example of the first approach is the extensive survey of two-component, spherical, self-consistent galaxy models carried out by Bertin and coworkers (Bertin, Saglia, & Stiavelli 1992). They assumed for the stellar and dark matter components two distribution functions of the f_∞ form (and so positive by choice) (Bertin & Stiavelli 1984). The main problem with this approach is that generally the spatial density is not expressible in terms of known functions, and so only numerical investigations are feasible.

In the second approach, the density distribution is given and assumptions on the model internal dynamics are made, making comparison with the data simpler. But the difficulties inherent in the operation of recovering the DF in many cases prevent a simple consistency analysis. In particular, in order to recover the DF of spherical models with anisotropy, two techniques have been developed from the original Eddington (1916) method for isotropic systems: the Osipkov-Merritt (OM) technique (Osipkov 1979; Merritt 1985), and the case discussed by Cuddeford & Louis (1995, and references therein). Examples of *numerical* application of the OM inversion to two-component spherical galaxies can be found in the literature (see, e.g., Ciotti & Pellegrini 1992, hereafter CP92; Carollo, de Zeeuw, & van der Marel 1995). For axisymmetric systems, recently a new inversion technique, less restrictive than the classical ones (Lynden-Bell 1962; Hunter 1975; Dejonghe 1986), has been found (Hunter & Qian 1993). If one is just interested in the consistency of a stellar system, the previous methods yield "too much," i.e., the DF. A simpler approach, at least for spherically symmetric multicomponent systems with OM anisotropy—as the case discussed in this paper—is given by a method described by CP92, which requires information only on the radial density profiles of each component.

Despite all these efforts, a small number of one-component systems in which both the spatial density and the DF are analytically known is at our disposal, and in the more interesting case of two-component systems only the very remarkable axisymmetric Binney-Evans model is known (Binney 1981; Evans 1993). The result proved here, that also the DF of the superposition of two Hernquist density distributions (hereafter "HH models") with OM anisotropy is completely expressible in an analytical way, is therefore of particular interest. This family of models is made by the superposition of a stellar and a dark matter distribution, both following the Hernquist profile, with different total masses and core radii. The concentration and the amount of the stellar and dark matter distributions are described by four free parameters, and orbital anisotropy is allowed in both components, following the OM prescription. A particularly interesting case is obtained for a null core radius of the "halo," so mimicking a central black hole (BH). The study of HH models is also useful for many different reasons: to provide an analytical DF for a two-component cuspy system, for which the analytical solution of the Jeans equations is also available (Ciotti, Lanzoni, & Renzini 1996); to investigate the role of anisotropy and mass distribution of each component in determining the positivity of their DFs; to compute in an accurate and "easy" way the model line profiles in order to arrange initial conditions for numerical simulations of two-component systems.

In § 2, I briefly review the method presented in CP92, formulating it in a way suitable for its application to the present problem. Then in § 3, I introduce the HH models and use the previous method to discuss the limits imposed on their parameters by the positivity of the DFs of the two components. It is proved that globally isotropic HH models are consistent for any mass ratio and core radii ratio, even in the case of a central BH. In this last case, the analytical expression for a lower limit of the anisotropy radius of the host system as a function of the BH mass is given. In § 4, I derive the DF for HH models and their differential energy distribution in the case of global isotropy; some velocity sections of the DF are also shown. In the case of a dominant halo, it is found that the DF of an HH component can be expressed only through elementary functions. A particular case—corresponding to a Hernquist model with a central BH—is extensively discussed. In § 5, the exact boundary of the region of consistency in the parameter space is obtained by using the DF, and the results are compared with those given in § 3. In the same section, the stability of globally isotropic HH models is proved, and a discussion on the stability of the anisotropic case is given. Finally, in § 6, the main results are summarized.

2. THE CONSISTENCY OF MULTICOMPONENT SYSTEMS

More important than the construction of its spatial and projected velocity dispersion profile is checking whether a galaxy (or a galaxy cluster) model is consistent, i.e., is described by a DF that is everywhere nonnegative. If a system is described as a sum of different density components ρ_k, then *each* f_k must be nonnegative. This requirement leads us to introduce the concept of consistent multicomponent decomposition of a system, as discussed in CP92, together with the main theorem used here. This theorem permits us to check whether the DF of a multicomponent spherical system, where the orbital anisotropy of each component is described by the OM anisotropy, is positive, *without* calculating it effectively. In the OM formulation, the radially anisotropic case is obtained as a consequence of assuming that $f = f(Q)$ with

$$Q = \mathscr{E} - \frac{L^2}{2r_a^2}, \tag{1}$$

where $\mathscr{E}$ and L are respectively the relative energy and the angular momentum modulus per unit mass, $f(Q) = 0$ for $Q \le 0$, and r_a is the so-called *anisotropy radius*. With this assumption the models are characterized by radial anisotropy increasing with the galactic radius, and in the limit $r_a \to \infty$ the velocity dispersion tensor is globally isotropic. For a multicomponent spherical system, the simple relation between energy and angular momentum prescribed by equation (1) allows to express the DF of the kth component as

$$f_k(Q_k) = \frac{1}{\sqrt{8}\pi^2}\frac{d}{dQ_k}\int_0^{Q_k}\frac{d\varrho_k}{d\Psi_T}\frac{d\Psi_T}{\sqrt{Q_k - \Psi_T}} = \frac{1}{\sqrt{8}\pi^2}\int_0^{Q_k}\frac{d^2\varrho_k}{d\Psi_T^2}\frac{d\Psi_T}{\sqrt{Q_k - \Psi_T}}, \tag{2}$$

where

$$\varrho_k = \rho_k\left(1 + \frac{r^2}{r_{ak}^2}\right), \tag{3}$$

© American Astronomical Society • Provided by the NASA Astrophysics Data System

$\Psi_T(r) = \sum \Psi_k(r)$ is the relative total potential, $Q_k = \mathscr{E} - L^2/2r_{ak}^2$, and $0 \le Q_k \le \Psi_T(0)$. The second equivalence in equation (2) holds for untruncated systems with a finite total mass (see BT87, p. 240), as the HH models here discussed. The original theorem, given in CP92 in terms of the model radius, is here formulated in terms of the relative potential Ψ_k of the investigated component since this formulation makes the treatment of HH models easier.

THEOREM. *The necessary condition for the nonnegativity of f_k given in equation (2) is*

$$\frac{d\varrho_k}{d\Psi_k} \ge 0\,, \quad 0 \le \Psi_k \le \Psi_k(0)\,. \tag{4}$$

If this necessary condition is satisfied, a strong sufficient condition (SSC) for the nonnegativity of f_k is

$$\frac{d}{d\Psi_k}\left[\frac{d\varrho_k}{d\Psi_k}\left(\frac{d\Psi_T}{d\Psi_k}\right)^{-1}\sqrt{\Psi_T}\right] \ge 0\,, \quad 0 \le \Psi_k \le \Psi_k(0)\,. \tag{5}$$

Proof. See CP92.

Note that a *weak sufficient condition* (WSC),

$$\frac{d}{d\Psi_k}\left[\frac{d\varrho_k}{d\Psi_k}\left(\frac{d\Psi_T}{d\Psi_k}\right)^{-1}\right] \ge 0\,, \tag{6}$$

is obtained in a much easier way by using the last expression in equation (2), requiring that $d^2\varrho_k/d\Psi_T^2 \ge 0$. The WSC is obviously better suited than the SSC for analytical investigations because of the absence of the weighting square root of the total potential.

Some considerations follow by looking at the previous conditions. The first is that the violation of the necessary condition (eq. [4]) is connected only with the radial behavior of ρ_k and the value of r_{ak}, so this condition is valid *independently* of any other interacting component added to the model. Even when the necessary condition is satisfied, f_k can be negative, as a result of the radial behavior of the integrand in equation (2), which depends on the total potential, on the particular ρ_k, and on r_{ak}; some permitted values of r_{ak} satisfying the necessary condition must be discarded. Naturally, the true critical anisotropy radius is always larger than or equal to that given by the necessary condition and smaller than or equal to that given by the SSC and WSC. The previous analysis has been performed obtaining analytical or numerical limits on r_a for some widely used models: for example, in CP92, the King (1972), de Vaucouleurs (1948), and quasi-isothermal density distributions were discussed, and more recently the Jaffe (1983), Hernquist (H90), and Plummer (1911) distributions (Ciotti et al. 1996).

A complete analysis of the HH models is given in the next section, deriving the analytical constraints on r_a for (1) an H model and (2) an H model with a central BH, and finally (3) showing the consistency of the general HH model in the case of global isotropy.

3. THE HH MODELS

In the study of the HH models, some simplification arises from the fact that both components are described by the same functional form. So, I do not distinguish between "stars" and "dark matter," but simply between a *reference* system and a *halo* system. The mass M and the core radius r_c of the reference system are the normalization constants, so that its density distribution is

$$\rho(r) \equiv \rho_N \tilde{\rho}(s) = \frac{\rho_N}{s(1+s)^3}\,, \tag{7}$$

where $s = r/r_c$ and $\rho_N = M/2\pi r_c^3$ (H90). The halo density is described by another Hernquist distribution, of mass $M_h = \mu M$ and core radius $r_h = \beta r_c$:

$$\rho_h(r) = \frac{\rho_N \mu\beta}{s(\beta+s)^3}\,. \tag{8}$$

Then the HH density profiles are fully determined by fixing the four independent parameters (M, r_c, μ, β), with $0 \le \mu$ and $0 \le \beta$. Note that for $\mu = 0$ the HH models reduce to the H model and that for $\beta \le 1$ the halo density is more concentrated than the reference component.

The fundamental ingredient in recovering the DF is the relative potential Ψ, which for the reference component is

$$\Psi(r) \equiv \Psi_N \tilde{\Psi}(s) = \frac{\Psi_N}{1+s}\,, \quad 0 \le \tilde{\Psi} \le 1\,, \tag{9}$$

and for the halo is

$$\Psi_h(r) \equiv \Psi_N \tilde{\Psi}_h(s) = \frac{\Psi_N \mu}{\beta+s}\,, \tag{10}$$

with $\Psi_N = GM/r_c$ (H90). Note how, for $\beta = 0$, the halo potential is that of a BH of mass M_h placed at the center of the reference system. As will become clear in § 4, a fundamental property of HH models is that their total potential can be expressed as a simple function of the reference potential, namely,

$$\tilde{\Psi}_T = \tilde{\Psi}\left(1 + \frac{\mu}{1+b\tilde{\Psi}}\right), \quad b \equiv \beta - 1 \ge -1\,, \tag{11}$$

where the interval $0 \le \tilde{\Psi} \le 1$ is monotonically mapped onto $0 \le \tilde{\Psi}_T \le 1 + \mu/\beta$.[1]

3.1. *The Necessary and Sufficient Conditions for the H Model*

Here I apply first the necessary condition to the H model to determine the *critical* anisotropy radius such that a higher degree of radial OM anisotropy produces a negative DF, no matter what kind of halo density distribution is added. The first step is to express the modified density ϱ (see eq. [3]) as a function of the relative potential $\tilde{\Psi}$, obtaining

$$\tilde{\varrho}(\tilde{\Psi}) = \frac{\tilde{\Psi}^4}{1-\tilde{\Psi}}\left[1 + \frac{(1-\tilde{\Psi})^2}{s_a^2\tilde{\Psi}^2}\right], \tag{12}$$

where $s_a = r_a/r_c$ is the dimensionless anisotropy radius.

As shown in Appendix A (eqs. [A1]–[A2]), the necessary condition can be treated analytically, requiring

$$s_a \ge \sqrt{\frac{(3\tilde{\Psi}_M - 2)}{(4 - 3\tilde{\Psi}_M)}}\,\frac{(1-\tilde{\Psi}_M)}{\tilde{\Psi}_M} \simeq 0.128\,, \tag{13}$$

where $\tilde{\Psi}_M$ is the value of the potential for which the right-hand side of equation (A1) is maximum. In Figure 1, the solid line at the bottom represents the derived lower bound for the anisotropy radius.

[1] The case $b = 0$ (i.e., $\beta = 1$) is discarded from here on, it being the case of an H model of total mass $M(1+\mu)$, fully discussed in H90.

© American Astronomical Society • Provided by the NASA Astrophysics Data System

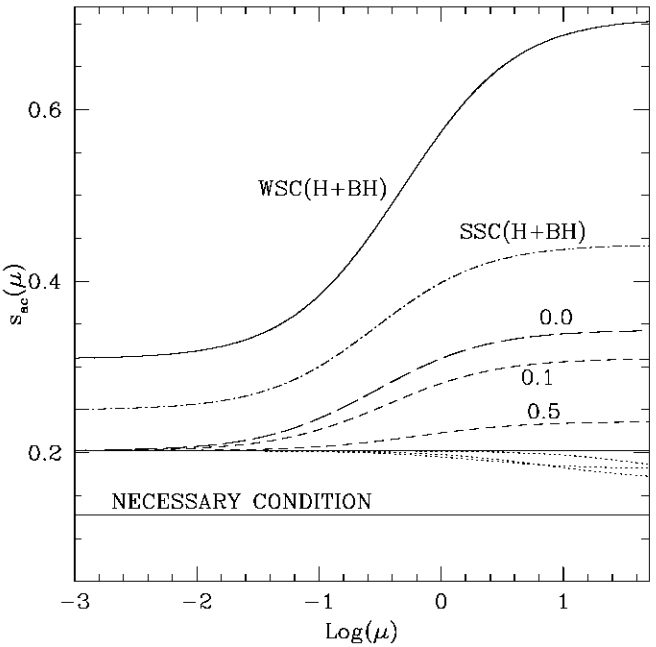

FIG. 1.—Limits on the anisotropy radius for the consistency of the reference component, for various (μ, β)-values. The lowest solid line is the necessary condition. The middle solid line is the minimum anisotropy radius for the H model. The dotted lines are the limits in the presence of a more extended halo, with $\beta = 2, 5, 20$. The short-dashed lines correspond to a halo with $\beta = 0.5, 0.1$, and the long-dashed lines to the case of the central BH. The dot-dashed and the uppermost solid line are the SSC and WSC, respectively, for the case of the central BH.

Moving to the study of the sufficient conditions, I apply first the SSC. The calculations can be performed analytically, and the result is

$$s_a \geq \sqrt{\frac{3(5\tilde{\Psi}_M - 2)(1 - \tilde{\Psi}_M)^3}{15\tilde{\Psi}_M^2 - 39\tilde{\Psi}_M + 28}} \frac{1}{\tilde{\Psi}_M} \simeq 0.25 \qquad (14)$$

[eqs. (A3)–(A5)], a limit obviously higher than that obtained from the necessary condition. The true limit on s_a for the H model is within the two previous values, and in fact its value determined directly from the DF is $\simeq 0.202$ (see § 4.2). In Figure 1, this value is represented by the middle solid line. The result of the application of the WSC to the H model will be obtained as a limiting case of the more general analysis in the next subsection.

3.2. *Sufficient Conditions for the H + BH and Isotropic HH Models*

In order to proceed further with this analytical discussion, and to consider the more complicated case of the presence of the halo, we need to use the WSC rather than the SSC, because of the presence of the square root of the total potential in the SSC. I now prove two important results:

1. In the case of an H + BH model (i.e., an H model with a central BH of mass μM), the WSC permits us to recover analytically a minimum value of the anisotropy radius as a function of the central BH mass.

2. *Globally isotropic* HH models can be consistently constructed for *any* value of (μ, β). In particular, this means that *a globally isotropic H model can consistently host a BH of any mass at its center.*

In the case of a central BH, the WSC prescribes that

$$s_a \geq \left[-\frac{3\tilde{\Psi}_M(\mu)^4 - 10\tilde{\Psi}_M(\mu)^3 + 6(2+\mu)\tilde{\Psi}_M(\mu)^2}{3\tilde{\Psi}_M(\mu)^2 - 8\tilde{\Psi}_M(\mu) + 6 + 6\mu} - \frac{6(1+\mu)\tilde{\Psi}_M(\mu) + (1+\mu)}{3\tilde{\Psi}_M(\mu)^2 - 8\tilde{\Psi}_M(\mu) + 6 + 6\mu} \right]^{1/2} \frac{1}{\tilde{\Psi}_M(\mu)} \qquad (15)$$

[eqs. (A6)–(A10)], corresponding to the uppermost solid line in Figure 1. As is intuitive, an increase of the BH mass produces an increase of the critical anisotropy radius, i.e., a decrease in the maximum value allowed for the radial anisotropy. Two interesting consequences can be obtained by performing the asymptotic analysis of the previous equation, for $\mu \to \infty$ and $\mu \to 0$.

The asymptotic behavior of equation (15) for $\mu \to \infty$ is $s_a(\mu) \geq 1/\sqrt{2} + O(1/\mu)$, and so just a slight reduction in anisotropy with respect to the one-component model is required by the presence of a BH of any mass; the finite value of $s_a(\infty)$ implies that a globally isotropic model can host a central BH of any mass. The limiting case of the previous analysis for $\mu = 0$ is the WSC applied to the H model and completes the discussion given in § 3.1. The limit for $\mu \to 0$ of equation (15) is

$$s_a \geq \sqrt{\frac{(3\tilde{\Psi}_M - 1)(1 - \tilde{\Psi}_M)^3}{3\tilde{\Psi}_M^2 - 8\tilde{\Psi}_M + 6}} \frac{1}{\tilde{\Psi}_M} \simeq 0.31 , \qquad (16)$$

and comparison of this value with the limit on the anisotropy radius derived from the SSC ($s_a \geq 0.25$) is instructive: the difference is due to the weight factor of the square root of the potential, contained in the SSC and absent in the WSC. The numerical evaluation of the SSC in the case of a BH is very easy, and the result is plotted in Figure 1 (*dot-dashed line*).

A second interesting case for which the WSC can be treated analytically is that of a completely isotropic component of the HH model; in Appendix A, it is shown that its DF is positive for any choice of (μ, β). Incidentally, this provides another proof that it is always possible to couple consistently a BH of any mass with a globally isotropic H model, in accordance with the previous result.

4. THE DISTRIBUTION FUNCTION OF HH MODELS

After the preliminary discussion, we can now proceed to the explicit recovery of the DF. Because of the fact that both density components of the HH model are described by the same functional form, it suffices to compute the DF for the reference component with generic (μ, β), and then the DF for the halo component also is easily recovered. As for the density and the potential, for f it is also useful to work with dimensionless functions. So, for the reference component, $f = f_N \tilde{f}(\mu, \beta; \tilde{Q})$ with $f_N = \rho_N \Psi_N^{-3/2}$ and $0 \leq \tilde{Q} \equiv Q/\Psi_N \leq 1 + \mu/\beta$. For the halo component a similar functional form holds, where the two dimensional constants are now the mass and the core radius of the halo and the two dimensionless parameters are $\mu_h \equiv M/M_h = 1/\mu$ and $\beta_h \equiv r_c/r_h = 1/\beta$. The DF for the halo component is then obtained from that of the reference component by changing the normalization constant f_N to f_{Nh}, substituting the dimensionless

© American Astronomical Society • Provided by the NASA Astrophysics Data System

parameters (μ, β) with their inverses, and rescaling the parameter Q to the halo central potential.

The easiest way to compute the DF is to use the first of the identities in equation (2). For the evaluation of the integral, one would be tempted to express $\varrho(\Psi_T)$ by eliminating the radial coordinate from the modified density and the total potential; this can be formally done, but the resulting expression for the radius involves a quadratic irrationality, which after insertion in equations (3) and (7) produces an intractable expression. Here I follow another approach: instead of eliminating the radius, the variable of integration is changed from the total potential to the potential of the reference component. This is equivalent to a remapping of the domain of definition of the DF, from the range of variation of Ψ_T to the range of variation of Ψ, and leads to the introduction of a new parameter q, defined from equation (11) as

$$\tilde{Q} = q\left(1 + \frac{\mu}{1 + bq}\right), \quad 0 \le q \le 1 . \tag{17}$$

With this change of variable, the DF is given by equations (B1)–(B3), but as shown subsequently in Appendix B, this is again *not* the *natural* parameterization for f, which is finally obtained by defining the variable

$$l^2 \equiv 1 + bq . \tag{18}$$

After normalizing to the dimensional scales of the reference component, its DF can be formally written as

$$f(Q) \equiv f_i(Q) + \frac{f_a(Q)}{s_a^2} = \frac{f_N}{\sqrt{8}\pi^2}\left(\frac{d\tilde{Q}}{dl}\right)^{-1} \times \frac{d}{dl}\left[\tilde{F}_i^{\pm}(l) + \frac{\tilde{F}_a^{\pm}(l)}{s_a^2}\right], \quad l = l^{-1}(\tilde{Q}) , \tag{19}$$

where the subscripts refer to the isotropic and anisotropic parts of the DF, respectively, and

$$\frac{d\tilde{Q}}{dl} = 2\,\frac{l^4 + \mu}{bl^3} . \tag{20}$$

The superscript plus or minus in equation (19) corresponds to the cases $b > 0$ and $-1 \le b < 0$, respectively, and $\tilde{F}_i^{\pm}(l)$ and $\tilde{F}_a^{\pm}(l)$ are given in Appendix B. Note how, with this procedure, $f(Q)$ results from the elimination of the parameter q between equations (17) and (18)–(19). A first (but algebraically cumbersome) check of the derived formula is obtained by evaluating analytically its limit for $\mu = 0$ and recovering the DF of the H model given by H90. The lengthy proof is not presented here. In the general case of $\mu > 0$, a check is obtained by confrontation of the analytical DF with that derived by direct numerical inversion of equation (2); the two families of curves are indistinguishable, with percentage errors smaller than 10^{-5}.

In Figure 2 (*top*), some DFs are shown in the case of global isotropy. Their main characteristic is that, when the halo is more extended than the reference component (*dotted lines*), they are more peaked than the DF of the H model (*solid line*). On the contrary, for halos more concentrated than the reference component (*short-dashed lines*), the DFs are flatter. A particular case is that corresponding to a central BH (*long-dashed lines*): the DFs are positive—as discussed in § 3.2—but *not* monotonically increasing near the model center. In the bottom panel of Figure 2, the DFs for the same models above are shown, but in this case the anisotropy radius is fixed at $s_a = 1$. The same qualitative comments as in the isotropic case apply.

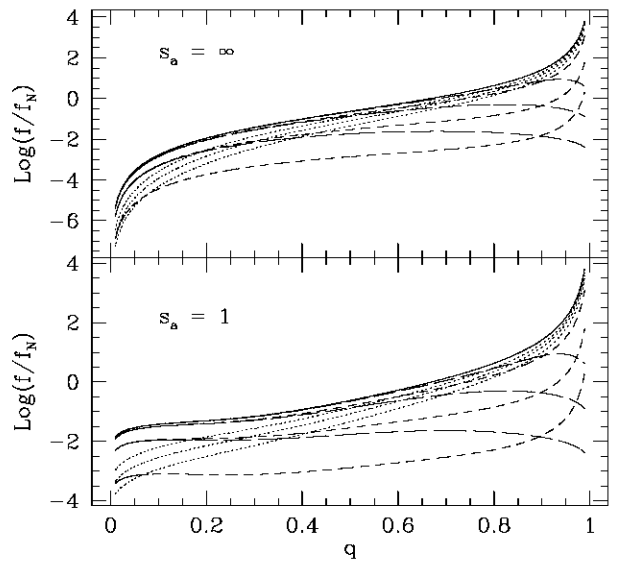

FIG. 2.—*Top*: DFs for the reference component of the HH models in case of global isotropy. The solid line is the DF of the H model. The dotted lines correspond to the DF in presence of a halo more extended than the reference component, with $\beta = 5$, and $\mu = 5$, 10, 20. The short-dashed lines refer to a more concentrated halo, with $\beta = 0.2$, and with masses $\mu = 0.1$, 1, 10. Finally, the long-dashed lines correspond to a central BH, of masses $\mu = 0.01$, 0.1, 1. *Bottom*: DFs for the reference component of the HH model in the case of radial anisotropy with $s_a = 1$. The several curves correspond to the same parameters as in the isotropic case.

An important feature of Figure 2 is the radically different behavior of f for $q \to 1$: while for any finite core radius of the halo the DF of the reference component diverges near the center, in the presence of a central BH the DF converges, i.e., the DF for the BH case cannot be obtained *directly* as a limit for $\beta \to 0$ of the DF with $\beta > 0$. The discontinuity in the DF's behavior at high energies is due to the discontinuity of the functions X_1 and X_2 in equation (B12): as a consequence, the two limits $\beta \to 1$ and $l^2 \to \beta$ cannot be interchanged. The derivation of the DF for the BH case from the DF with $\beta > 0$ is described in Appendix B (§ B2).

A more direct way to look at this discontinuity is to perform an asymptotic expansion of the DF for $q \to 1$. A brute force (and highly error-prone) approach would be the expansion of the expressions given in Appendix B for $q \to 1$, but a cleaner asymptotic expansion can be obtained by instead directly expanding equations (B1)–(B3); for $\beta > 0$, the leading term is

$$\tilde{f}(q) \sim \frac{3}{8\sqrt{2}\pi}\,\frac{[1 + (\beta - 1)q]^2}{\mu + [1 + (\beta - 1)q]^2} \times \frac{\beta}{\sqrt{\mu + \beta^2}(1 - q)^{5/2}}, \quad q \to 1 . \tag{21}$$

The order of divergency, also in presence of the halo, is equal to that given in H90, and assuming that $\mu = 0$ or

© American Astronomical Society • Provided by the NASA Astrophysics Data System

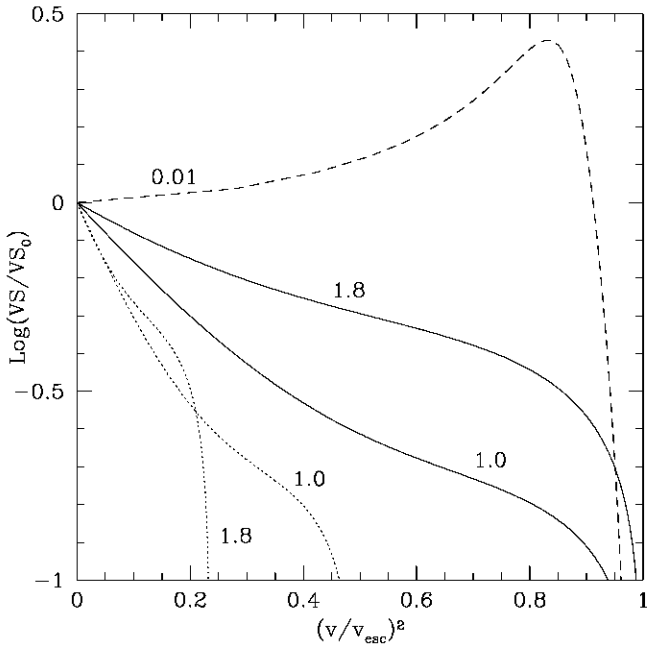

FIG. 3.—Radial (*solid lines*) and tangential (*dotted lines*) normalized velocity sections for the H model, with $s_a = 1$. The numbers near the lines give the normalized radius at which the section is shown. The dashed line is the section at $r/r_c \simeq 0.01$ in the case of a central BH with $\mu = 0.1$.

$\beta = 1$, the correct asymptotic formula for the H model is recovered.[2]

Consistent with the previous discussion, the asymptotic formula for $q \to 1$ in the case of a central BH *cannot* be obtained as the limiting case of the previous formula when $\beta = 0$, because of a change in the order of the singularity in equation (B2). The correct treatment in this case yields

$$\tilde{f}(q) \sim \frac{1}{2\pi^2\sqrt{2\mu q}} \frac{\sqrt{1-q}}{\mu + (1-q)^2}, \quad q \to 1, \qquad (22)$$

and the convergence to 0 of the DF is proved. Finally, note how the presence of anisotropy does not affect the behavior of the DF for high relative energies, as dictated by equation (12), from which it can be easily seen that the divergence of the modified density near the model center—the leading term in the asymptotic expansion of the DF—is only due to its isotropic part. The asymptotic formulae (21)–(22) have been checked numerically for many choices of (μ, β) by direct comparison with the DF, and the agreement is excellent.

4.1. *Velocity Sections of the DF*

The representation of the DF as a function of the integral of motion Q is not easily interpreted when orbital anisotropy is present. More intuitive are the *velocity sections* of f, i.e., for some fixed r, the distributions of v_r and v_t, the radial and tangential velocity components, respectively. In Figure 3, the sections $f(r, v_r, 0)$ and $f(r, 0, v_t)$ for the H model with $s_a = 1$ are shown. Obviously, for global isotropy the two distributions are equal, and for anisotropic systems they become more and more similar moving from radii greater than r_a to smaller radii, according to the radial trend of anisotropy implied by the OM parameterization. As expected, for a finite value of r_a, when moving outward the tangential orbits become more and more depopulated, and this is compensated by an increase in the number of high-velocity radial orbits. The presence of a massive diffuse halo does not qualitatively alter the distributions, which maintain the same aspect. The only peculiar characteristic appears again in the case of the central BH, when the maximum of the distribution is placed off-center: this fact reflects the central behavior of the DF described previously. As a final and general remark on these sections, one can note how they depart appreciably from a Maxwellian distribution.

4.2. *The Differential Energy Distribution of HH Models*

In the case of global isotropy, the differential energy distribution $dM/d\mathscr{E}$ for each component of the HH models can be derived analytically as a function of the parameter l. As shown by BT87 (p. 243), $dM/d\mathscr{E} = f(\mathscr{E})g(\mathscr{E})$, where

$$g(\mathscr{E}) = 16\sqrt{2}\pi^2 g_N \tilde{G}^{\pm}(l) \qquad (23)$$

is the density of states and $g_N = r_c^3 \Psi_N^{1/2}$. The explicit form for $\tilde{G}^{\pm}(l)$ is given in Appendix C, and the superscript plus or minus corresponds to the cases $b > 0$ and $-1 \le b < 0$, respectively. Again, a first check of the derived formula can be obtained by evaluating analytically its limit for $\mu = 0$ and recovering the $g(\mathscr{E})$ as given by H90; as in the case of the DF, the proof is cumbersome and is not shown here. When also a halo is present, the check is obtained by direct comparison with the density of states derived by numerical integration of equation (C2). Over the whole energy range, the curves are indistinguishable. In Figure 4, $dM/d\mathscr{E}$ is plotted; when the halo is more extended than the reference component ($\beta > 1$, *dotted lines*), $dM/d\mathscr{E}$ is no longer steadily increasing in the outer part of the system.

4.3. *The DF for Halo-dominated HH Models*

In the case of a halo-dominated model, i.e., when the self-gravity of the reference component is negligible, the DF

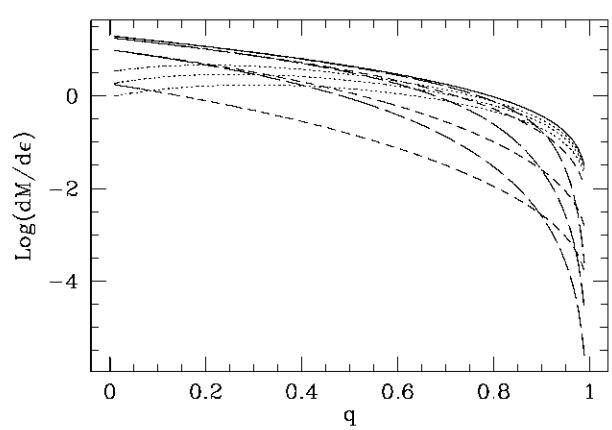

FIG. 4.—Differential energy distribution for the reference component in the case of global isotropy. The solid line is the $dM/d\mathscr{E}$ of the H model. The other lines correspond to the same parameters described in Fig. 2.

[2] All the higher order terms in eqs. (21)–(22) can written explicitly, but their expressions become increasingly complicated. Note that eq. (21) of H90 is incorrect, as can be shown by expanding eq. (17) there. Note also that the parameter q used in H90 is the square root of the parameter used in this paper.

© American Astronomical Society • Provided by the NASA Astrophysics Data System

and $dM/d\mathscr{E}$ can be expanded for $\mu \to \infty$, and the resulting expressions are combinations of elementary functions of l. For brevity, and because of its major importance, only the explicit forms of the functions entering the DF are presented.

4.3.1. *The Case* $\beta > 1$

In this case, $\tilde{F}_i^+$ and $\tilde{F}_a^+$ are given by equations (B8)–(B9), with

$$C_6(l) = \frac{5}{16}\arccos\left(\frac{1}{l}\right) + \sqrt{l^2-1}\left(\frac{5}{16l^2} + \frac{5}{24l^4} + \frac{1}{6l^6}\right), \tag{24}$$

$$C_4(l) = \frac{3}{8}\arccos\left(\frac{1}{l}\right) + \sqrt{l^2-1}\left(\frac{3}{8l^2} + \frac{1}{4l^4}\right), \tag{25}$$

$$C_2(l) = \frac{1}{2}\arccos\left(\frac{1}{l}\right) + \frac{\sqrt{l^2-1}}{2l^2}, \tag{26}$$

$$V_1(\beta, l) = \sqrt{\frac{\beta - l^2}{\beta}}\arctan\sqrt{\frac{\beta(l^2-1)}{\beta - l^2}}, \tag{27}$$

$$V_2(\beta, l) = \frac{(2\beta - l^2)V_1(\beta, l)}{2\beta} + \frac{(\beta - l^2)\sqrt{l^2-1}}{2\beta(\beta-1)}. \tag{28}$$

4.3.2. *The Case* $0 \le \beta < 1$

In this case, $\tilde{F}_i^-$ and $\tilde{F}_a^-$ are given by equations (B12)–(B13), with

$$D_6(l) = \frac{5}{16}\operatorname{arccosh}\left(\frac{1}{l}\right) + \sqrt{1-l^2}\left(\frac{5}{16l^2} + \frac{5}{24l^4} + \frac{1}{6l^6}\right), \tag{29}$$

$$D_4(l) = \frac{3}{8}\operatorname{arccosh}\left(\frac{1}{l}\right) + \sqrt{1-l^2}\left(\frac{3}{8l^2} + \frac{1}{4l^4}\right), \tag{30}$$

$$D_2(l) = \frac{1}{2}\operatorname{arccosh}\left(\frac{1}{l}\right) + \frac{\sqrt{1-l^2}}{2l^2}, \tag{31}$$

$$X_1(\beta, l) = \sqrt{\frac{l^2 - \beta}{\beta}}\arctan\sqrt{\frac{\beta(1-l^2)}{l^2 - \beta}}, \tag{32}$$

$$X_2(\beta, l) = \frac{(2\beta - l^2)X_1(\beta, l)}{2\beta} + \frac{(\beta - l^2)\sqrt{1-l^2}}{2\beta(\beta-1)}. \tag{33}$$

In the particular case of a dominating central mass, the DF is obtained by setting $\beta = 0$ in equations (B12)–(B13), eliminating the term containing X_2, and using equations (29)–(32) with $\lim_{\beta\to 0} X_1(\beta, l) = (1-l^2)^{1/2}$.

5. CONSISTENCY OF HH MODELS

We can now explore the parameter space of HH models, studying numerically the formulae derived in § 4. The simplest way to summarize the results is to express the consistency limitations in terms of the (normalized) anisotropy radius of the reference component. This is particularly indicated because (1) we know from the introductory discussion (§ 3.2) that the globally isotropic component of the HH model is consistent whatever the halo component is (i.e., $f_i > 0$) and, (2) in the case of the OM anisotropy, the anisotropy radius can be isolated in the DF. So, in the parameter space (s_a, μ, β), it is easy to determine the critical value $s_{ac}(\mu, \beta)$ defined as the anisotropy radius such that for $s_a < s_{ac}$ there exists at least one permitted value of the potential for which $f < 0$. Imposing the positivity of f over all the domain $0 < q < 1$, from equation (19) one obtains

$$s_{ac}^2(\mu, \beta) = \sup\left[-\frac{f_a(q)}{f_i(q)}\right]_{q\in(0,1)}. \tag{34}$$

In Figure 1, different curves s_{ac}^2 are plotted, for a varying halo mass, and for fixed values of β. As expected, no model permits a smaller value of the anisotropy radius than that derived from the necessary condition. The intermediate solid line is the value of the exact limit on the anisotropy radius for the H model, $s_a \simeq 0.202$. The upper solid curve is the plot of the WSC in the case of a central BH of normalized mass μ. As described in § 3.2, this curve approaches asymptotically the value $1/\sqrt{2}$.

The dashed and dotted lines represent the lower bound on the anisotropy radius for various β. Clearly, all the families of curves for $\mu \to 0$ converge to the value required by the H model. The first result is that the critical anisotropy radius for each model is not strongly dependent on the halo mass, and it is always contained between the value given by the necessary condition and that obtained from the SSC applied to the H + BH model. The second result is that all models with $0 \le \beta < 1$ (*short-dashed lines*) have a critical anisotropy radius higher than the H model; as expected, a model with a concentrated halo cannot also sustain too much anisotropy. The long-dashed line represents the case of a central BH: anisotropy radii higher than the values represented by this curve can be assumed independently of the halo structure and mass. The third result is that all models in which the halo is more extended than the reference component can have a slightly smaller anisotropy radius than the H model, but in this case the effect is much less strong than for a $\beta < 1$ halo; as already found in CP92, the most diffuse component of a multicomponent system is also the most "delicate" concerning the consistency. Finally, note how all the curves become flat asymptotically. Their limiting value cannot be obtained directly by use of equation (19) for very high μ-values, as a result of the numerical precision loss of the intervening functions. On the contrary, a very accurate analysis can be performed by using the asymptotic functions given in § 4.3, and the result is plotted in Figure 5.

5.1. *Stability of HH Models*

As important as the discussion of the consistency of HH models is the location of the region of *stability* for such systems. A complete stability analysis is beyond the task of this work, requiring N-body simulations or normal-mode analysis, but some interesting conclusions can be equally derived, at least for the globally isotropic case. In fact in this case powerful theorems are at our disposal: for stability against both radial and nonradial perturbations, it is sufficient (but not necessary!) that the system DF (in our case the sum of the DFs of the halo and of the reference component) is an increasing function of the relative binding energy $\mathscr{E}$ (see, e.g., BT87, pp. 296–307; Fridman & Poliachenko 1984, pp. 152–163).

In the performed numerical exploration of the parameter space (μ, β), all the DFs *with* $\beta > 0$ are monotonically increasing functions of the parameter q, as shown for some particular cases in Figure 2. Changing the parameter q of

© American Astronomical Society • Provided by the NASA Astrophysics Data System

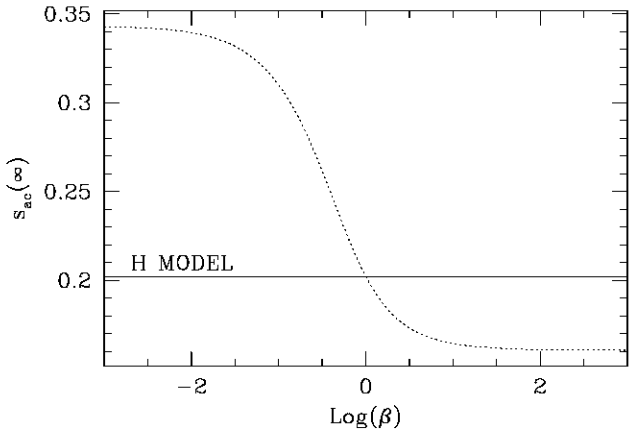

FIG. 5.—Minimum value for the anisotropy radius in the case of a dominant halo. Note the qualitative difference moving from a less extended halo to a more extended halo than the reference component.

each component to $\mathscr{E}$ using equation (17) and taking the derivative shows that the *globally isotropic HH models are stable*. Unfortunately, the sufficient condition above cannot be applied to the globally isotropic case with a central BH: the condition $df/d\mathscr{E} > 0$ is not verified, as a result of the convergence of the DF to 0, and so only numerical investigations can answer this interesting problem.

For anisotropic systems the situation is more complex, for the lack of general theorems. In any case, some hint can be obtained by the empirical requirement that $\xi \equiv 2K_{\rm rad}/K_{\rm tan} \lesssim \xi_c = 1.7 \pm 0.25$ (Fridman & Poliachenko 1984, p. 235) in order to avoid the radial orbit instability, where $K_{\rm rad}$ and $K_{\rm tan}$ are the total radial and tangential kinetic energies of the system, and the exact value of ξ_c is model dependent. A second complication with the previous criterion arises from the fact that a generalization to multicomponent systems is not obvious, as shown by Stiavelli & Sparke (1991). In that same paper, the authors showed with the aid of N-body simulations that the presence of a halo does not change very much the situation with respect to the one-component model. For HH models with OM anisotropy, the evaluation of $K_{\rm rad}$ and $K_{\rm tan}$ can be accomplished analytically, but the resulting formulae for $\beta > 0$ are complicated. For these reasons, I show here only the trend of the parameter $\xi(s_a, \mu)$ for the particular case of the H + BH system; the simpler case of an H model is obtained for $\mu = 0$. From the virial theorem, $K_{\rm rad} + K_{\rm tan} = (|U| + |W|)/2$, where U is the gravitational energy of the H model, W is its interaction energy with the BH, and so $\xi = 2/[(|U| + |W|)/2K_{\rm rad} - 1]$. Choosing as the energy normalization $U_N = M\Psi_N$, it results that $U = -2\pi \int \rho\Psi r^2\, dr = -U_N/6$, $W = 4\pi \int r^2 \rho (d\Psi_\mu/dr) dr = -U_N \mu$, and $K_{\rm rad} = 2\pi \int \rho \sigma_r^2 r^2\, dr = U_N(\tilde{K}^{\rm H}_{\rm rad} + \mu \tilde{K}^{\rm BH}_{\rm rad})$, with

$$\tilde{K}^{\rm H}_{\rm rad} = \frac{1 + 8s_a^2 + 23s_a^4 + 12s_a^6}{12(1 + s_a^2)^2} + \frac{\pi s_a(-1 + 16s_a^2 + 15s_a^4 + 6s_a^6)}{24(1 + s_a^2)^3} + \ln(s_a) s_a^3 \left[\frac{s_a(7 + 8s_a^2 + 3s_a^4)}{3(1 + s_a^2)^3} + \frac{\pi}{2} + \arctan s_a\right] - \frac{s_a^3[\pi \ln(1 + s_a^2) + s_a \Phi(-s_a^2, 2, 1/2)]}{4}, \quad (35)$$

$$\tilde{K}^{\rm BH}_{\rm rad} = \frac{12s_a^2 + 1}{2} + \frac{\pi s_a(2 + 3s_a^2)}{2(1 + s_a^2)} + \ln(s_a) s_a \left[\frac{s_a(5 + 6s_a^2)}{1 + s_a^2} + (1 + 6s_a^2)\left(\frac{\pi}{2} + \arctan s_a\right)\right] - \frac{s_a(1 + 6s_a^2)[\pi \ln(1 + s_a^2) + s_a \Phi(-s_a^2, 2, 1/2)]}{4}. \quad (36)$$

I have used for $\sigma_r^2(r)$, required in the integration, the expression given in Ciotti et al. (1996) (eqs. [A1]–[A3]), and the function Φ is the Lerch transcendent (see, e.g., Erdély et al. 1953, Vol. 1, p. 27). In Figure 6, the function ξ is plotted for various μ-values, and the asymptotic flattening to unity for increasing isotropy is evident. The first comment is that the stability criterion requires, also in the conservative hypothesis of a very high value of ξ_c (i.e., $\simeq 2.5$), minimum anisotropy radii appreciably larger than those obtained form the consistency analysis. For example, the minimum anisotropy radius permitted for an H model is $\simeq 0.93$, much higher than the value required by simple consistency, $\simeq 0.2$. So it is likely that the more radially anisotropic HH models with positive DF are with any probability radial orbit instability–prone. Another important comment concerns the relation between the relative distribution of the halo and of the reference component. As can be seen from Figure 6, halos more extended than the reference component make the model more unstable; on the contrary, more stable systems are obtained for more concentrated halos. This is easily explained by looking at the radial trend of the velocity dispersion as a function of the anisotropy radius. For extended halos, the velocity dispersion is mainly increased in the outer parts of the model, where the orbits are also strongly radial, and this correspondingly increases the ξ-

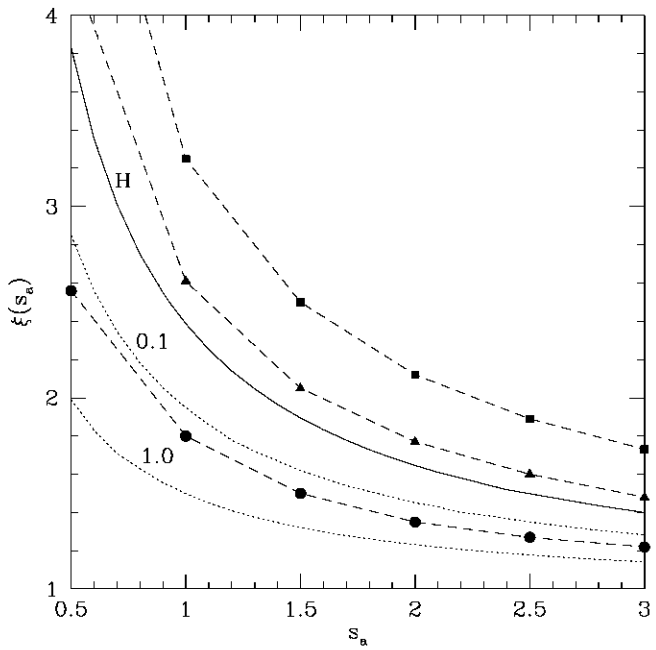

FIG. 6.—Value of the stability parameter for the reference component as function of the anisotropy radius. The solid line refers to the H model, and the dotted lines to H + BH models; the numbers are the μ-values. The other lines are the value of the stability parameter for various values of (μ, β): (1, 0.1) (*circles*), (10, 1.5) (*triangles*), and (10, 5) (*squares*).

© American Astronomical Society • Provided by the NASA Astrophysics Data System

value; the opposite happens for very concentrated halos. Particularly explicit are the two lines in Figure 6 that refer to a central BH: in this case, the velocity dispersion is essentially increased only at the model center, where isotropy is nearly realized, and the stability indicator remains low also for small values of r_a. But in this case the global indicator ξ probably loses its meaning because of a very strong *decoupling* between the central and the outer parts of the model.

6. CONCLUSIONS

In this paper an extensive analytical investigation of two-component spherical galaxy (or cluster) models, made of the sum of two Hernquist density distributions with different physical scales, was carried out. A variable amount of orbital anisotropy is also allowed in both components. These models, characterized by a power-law density profile in their central regions—both in the visible and in the dark matter distribution—reproduce the main properties of early-type galaxies as revealed by *Hubble Space Telescope* observations and also properties of the dark matter distribution as obtained in recent N-body simulations. The main results presented in this paper can be summarized as follows:

1. The analytical expression for the DF of HH models with general OM anisotropy is presented and discussed, even for the particular case of a Hernquist model with a central BH. The special case of a dominant dark halo is also discussed, and it is shown that under this assumption the DF can be asymptotically expressed using just elementary functions. In the case of global isotropy, the analytical expression for the differential energy distribution of both components is obtained. Some velocity sections of the DF are shown and discussed.

2. The necessary and sufficient conditions that the model parameters must satisfy in order to correspond to a consistent system (i.e., a system for which each physically distinct component has a positive DF) are analytically derived using the method introduced in CP92. It is proved that globally isotropic HH models are consistent for any mass ratio and core radii ratio, even in the special case in which the "halo" reduces to a BH. In the case of a central BH and of variable anisotropy for the host system, the analytical expression for a minimum anisotropy radius as a function of the BH mass is given.

3. The region in the parameter space in which HH models are consistent is subsequently explored using the DF. The main result is that the presence of a massive halo does not affect significantly the maximum anisotropy that can be sustained by a consistent model. It is shown that the presence of a halo with a core radius larger than that of the reference component allows a slightly higher degree of anisotropy with respect to the one-component Hernquist model. On the contrary, a halo with a smaller core radius imposes a larger value for the minimum anisotropy radius than that proper of the H model. The most restrictive case is that of a central BH. In any case, for a given core radius of the halo, there is a lower limit to the minimum anisotropy radius that approaches an asymptotic value for a dominant halo mass.

4. Finally, it is proved that isotropic HH models are stable, except for the case of a central BH, for which no conclusions can be drawn. For anisotropic models the stability parameter against radial orbit instability is briefly discussed, and it is shown that with high probability the most anisotropic *consistent* HH models are unstable.

I would like to thank Giuseppe Bertin and Silvia Pellegrini for helpful comments and discussions. This work has been partially supported by the Italian Ministry of Research (MURST).

APPENDIX A

CONSISTENCY REQUIREMENTS

In this appendix, I apply the CP92 method to the HH models, as discussed in § 3. The necessary condition for the H model imposes through equation (4) a limitation on the anisotropy radius:

$$s_a^2 \geq \frac{(3\tilde{\Psi}-2)(1-\tilde{\Psi})^2}{(4-3\tilde{\Psi})\tilde{\Psi}^2}, \qquad 0 \leq \tilde{\Psi} \leq 1. \tag{A1}$$

The requirement is that s_a^2 be larger than or equal to the maximum of the function on the right-hand side. This is reached at

$$\tilde{\Psi}_M = \frac{5}{4} - \frac{\sqrt{33}}{12} \simeq 0.77, \tag{A2}$$

which, after back-substitution in equation (A1), yields equation (13).

The SSC applied to the H model yields the following inequality:

$$s_a^2 \geq \frac{3(5\tilde{\Psi}-2)(1-\tilde{\Psi})^3}{(15\tilde{\Psi}^2-39\tilde{\Psi}+28)\tilde{\Psi}^2}, \qquad 0 \leq \tilde{\Psi} \leq 1. \tag{A3}$$

After differentiation, discarding the two complex conjugates roots of the resulting cubic equation, and defining

$$\phi_0 = \left(\frac{1336}{3645} + \frac{\sqrt{35887965}}{16200}\right)^{1/3}, \tag{A4}$$

© American Astronomical Society • Provided by the NASA Astrophysics Data System

the maximum of the right-hand side of equation (A3) is reached at

$$\tilde{\Psi}_M = \frac{23}{18} + \frac{217}{1620\phi_0} - \phi_0 \simeq 0.52 , \tag{A5}$$

which after back-substitution in equation (A3) yields equation (14).

The WSC applied to the H + BH model is obtained from equation (6) with $b = -1$. The inequality to be verified for a given μ is

$$s_a^2 \geq -\frac{3\tilde{\Psi}^4 - 10\tilde{\Psi}^3 + 6(2+\mu)\tilde{\Psi}^2 - 6(1+\mu)\tilde{\Psi} + (1+\mu)}{(3\tilde{\Psi}^2 - 8\tilde{\Psi} + 6 + 6\mu)\tilde{\Psi}^2} , \qquad 0 \leq \tilde{\Psi} \leq 1 . \tag{A6}$$

Taking the derivative of the right-hand side, we are left with the discussion of a rational function whose denominator is strictly positive and whose numerator is a polynomial of fifth degree, which fortunately can be factorized in a term of second degree strictly positive, and the cubic

$$c_\mu(\tilde{\Psi}) = -\tilde{\Psi}^3 + 4\tilde{\Psi}^2 - 6(1+\mu)\tilde{\Psi} + 2(1+\mu) . \tag{A7}$$

Observing that $c_\mu(0) = 2(1+\mu) > 0$ and $c_\mu(1) = -(1+4\mu)$, there is at least one solution of $c_\mu(\tilde{\Psi}) = 0$ between 0 and 1. This solution is also the only one, because the determinant of the cubic c_μ,

$$\Delta_\mu = 4(1+\mu)(216\mu^2 + 99\mu + 11)/27 , \tag{A8}$$

is positive for all $\mu \geq 0$; from the theory of algebraic equations, $c_\mu(\tilde{\Psi}) = 0$ admits one and only one real solution. Finally, considering the sign of c_μ, we proved that the solution $\tilde{\Psi}_M$ corresponds to a maximum. Defining

$$\phi_\mu = \left[\frac{\sqrt{3(1+\mu)(216\mu^2 + 99\mu + 11)}}{9} - 3\mu - \frac{17}{27}\right]^{1/3} , \tag{A9}$$

one obtains

$$\tilde{\Psi}_M(\mu) = \frac{4}{3} - \frac{2(1+9\mu)}{9\phi_\mu} + \phi_\mu , \tag{A10}$$

which after substitution in equation (A6) yields equation (15). When $\mu = 0$, the value at which the maximum is reached can be calculated directly from equations (A9)–(A10), obtaining

$$\phi_0 = \left(\frac{\sqrt{33}}{9} - \frac{17}{27}\right)^{1/3} , \tag{A11}$$

$$\tilde{\Psi}_M = \frac{4}{3} - \frac{2}{9\phi_0} + \phi_0 \simeq 0.456 , \tag{A12}$$

which after substitution in equation (A6) with $\mu = 0$ yields equation (16).

The application of the WSC to the globally isotropic HH models is more complicated. After having computed the derivatives in equation (6), we have to investigate the positivity of a rational expression, whose denominator is strictly positive for all $b \geq -1$ ($b \neq 0$), for all $\mu \geq 0$, and for $0 \leq \tilde{\Psi} \leq 1$. The numerator of this function factorizes in a strictly positive function and in the polynomial

$$\mu c_b(\tilde{\Psi}) + (3\tilde{\Psi}^2 - 8\tilde{\Psi} + 6)(1 + b\tilde{\Psi})^3 \geq 0 , \tag{A13}$$

where

$$c_b(\tilde{\Psi}) = 6b\tilde{\Psi}^3 + 3(1-5b)\tilde{\Psi}^2 + 2(5b-4)\tilde{\Psi} + 6 . \tag{A14}$$

It is trivial to show that the second addend of equation (A13) is strictly positive. I prove now that also c_b is positive for $b \geq -1$ and for $0 \leq \tilde{\Psi} \leq 1$, so the WSC is satisfied for any choice of (μ, β) and the globally isotropic HH models are consistent. First of all, $c_b(0) = 6$ and $c_b(1) = b + 1 = \beta \geq 0$, and so after excluding the presence of roots of c_b in the interval [0, 1], the proof is obtained. This can be accomplished by using the classical Sturm method, i.e., counting the differences in the number of variations between 0 and 1 in the Sturm sequence S_b associated with $c_b(\tilde{\Psi})$ and discussing it as a function of the parameter b. But a faster proof can be obtained as follows: Since c_b does not change sign between 0 and 1, only an *even* number of roots can be contained in the interval. If we show that equation (A14) admits only one real solution, then the proof is obtained. The discriminant of c_b,

$$\Delta_b = \frac{(125b^2 + 50b + 6)(b+1)^2}{2916b^4} , \tag{A15}$$

is strictly positive, so the cubic equation admits one and only one real solution, which is necessarily placed outside the interval [0, 1], and $c_b(\tilde{\Psi}) \geq 0$ for $0 \leq \tilde{\Psi} \leq 1$.

© American Astronomical Society • Provided by the NASA Astrophysics Data System

APPENDIX B

THE DISTRIBUTION FUNCTION FOR HH MODELS

In this appendix, the main analytical steps required for the determination of the DF are described. As discussed in § 4, the first step is to change the integration variable from the total potential to the potential of the reference component. After a normalization, equation (2) becomes

$$f(Q) = \frac{f_N}{\sqrt{8}\pi^2} \frac{d\tilde{F}[q(\tilde{Q})]}{d\tilde{Q}}, \tag{B1}$$

where the relation between q and $\tilde{Q}$ is given by equation (17) and

$$\tilde{F}(q) = \int_0^q \frac{d\tilde{Q}}{d\tilde{\Psi}} \frac{d\tilde{\Psi}}{\sqrt{\tilde{\Psi}_T(q) - \tilde{\Psi}_T(\tilde{\Psi})}}. \tag{B2}$$

From equations (11) and (17),

$$\tilde{\Psi}_T(q) - \tilde{\Psi}_T(\tilde{\Psi}) = \frac{(q - \tilde{\Psi})(\delta^2 + 1 + b\tilde{\Psi})}{1 + b\tilde{\Psi}}, \qquad \delta^2 \equiv \frac{\mu}{l^2}. \tag{B3}$$

It is shown in the following subsections that $\tilde{F}$ is actually a function of q only through l, defined by equation (18). Unfortunately its form changes depending on the sign of $b = \beta - 1$, and it is convenient to separate the discussion of the cases $\beta > 1$ and $0 \leq \beta < 1$.

B1. THE CASE $\beta > 1$

This is the simpler case, for which $b > 0$ and $1 \leq l^2 \leq \beta$. After the change of variable

$$t = \sqrt{1 + b\tilde{\Psi}}, \tag{B4}$$

equation (19) becomes

$$\tilde{F}^+(l) = \frac{2}{b^{5/2}} \int_1^l \left[\mathscr{R}_i(t) + \frac{\mathscr{R}_a(t)}{s_a^2}\right] \frac{dt}{\sqrt{(\delta^2 + t^2)(l^2 - t^2)}}. \tag{B5}$$

After a conversion in simple fractions, this results in

$$\mathscr{R}_a(t) = -3t^6 + 2(2 + \beta)t^4 - (1 + 2\beta)t^2, \tag{B6}$$

$$\mathscr{R}_i(t) = -3t^6 - 2(\beta - 4)t^4 - (\beta^2 - 4\beta + 6)t^2 - \frac{(\beta - 1)^4}{\beta - t^2} + \frac{\beta(\beta - 1)^4}{(\beta - t^2)^2}. \tag{B7}$$

Using the nomenclature of Byrd & Friedman (1971, hereafter BF71), we have

$$\tilde{F}_i^+(l) = \frac{2g}{b^{5/2}}\left[-3l^6C_6 - 2(\beta - 4)l^4C_4 - (\beta^2 - 4\beta + 6)l^2C_2 - \frac{(\beta - 1)^4}{\beta - l^2} V_1 + \frac{\beta(\beta - 1)^4}{(\beta - l^2)^2} V_2\right], \tag{B8}$$

and for the anisotropic part,

$$\tilde{F}_a^+(l) = \frac{2g}{b^{5/2}}\left[-3l^6C_6 + 2(\beta + 2)l^4C_4 - (1 + 2\beta)l^2C_2\right], \tag{B9}$$

where the functions $C_m(\phi, k)$ and $V_m(\phi, \alpha^2, k)$ are given in Appendix D, and

$$g = \frac{1}{\sqrt{\delta^2 + l^2}}, \qquad k^2 = \frac{l^2}{\delta^2 + l^2}, \qquad \phi = \arccos\left(\frac{1}{l}\right), \qquad \alpha^2 = \frac{l^2}{l^2 - \beta} \tag{B10}$$

(BF71, p. 48).

B2. THE CASE $0 \leq \beta < 1$

In this case, $\beta \leq l^2 \leq 1$. After the change of variable given in equation (B4), equation (19) becomes

$$\tilde{F}^-(l) = \frac{2}{|b|^{5/2}} \int_l^1 \left[\mathscr{R}_i(t) + \frac{\mathscr{R}_a(t)}{s_a^2}\right] \frac{dt}{\sqrt{(\delta^2 + t^2)(t^2 - l^2)}}. \tag{B11}$$

For the isotropic part,

$$\tilde{F}_i^-(l) = \frac{2g}{|b|^{5/2}}\left[-3l^6D_6 - 2(\beta - 4)l^4D_4 - (\beta^2 - 4\beta + 6)l^2D_2 - \frac{(\beta - 1)^4}{\beta - l^2} X_1 + \frac{\beta(\beta - 1)^4}{(\beta - l^2)^2} X_2\right], \tag{B12}$$

© American Astronomical Society • Provided by the NASA Astrophysics Data System

and for the anisotropic part,

$$\tilde{F}_a^-(l) = \frac{2g}{|b|^{5/2}} [-3l^6 D_6 + 2(\beta + 2) l^4 D_4 - (1 + 2\beta) l^2 D_2] , \tag{B13}$$

where the functions $D_m(\phi, k)$ and $X_m(\phi, \alpha^2, k)$ are given in Appendix D, and

$$g = \frac{1}{\sqrt{\delta^2 + l^2}} , \qquad k^2 = \frac{\delta^2}{\delta^2 + l^2} , \qquad \phi = \arccos l, \qquad \alpha^2 = \frac{\beta}{\beta - l^2} \tag{B14}$$

(BF71, p. 45).

The particular case of a central BH can be derived from the previous formulae. In this case $b = -1$ and so $0 \le l^2 \le 1$. The coefficients of the special functions are obtained from equations (B12)–(B13) for $\beta = 0$, and their arguments are still given by equation (B14). The only problem is in the isotropic part: the coefficient of X_2 is zero and $\lim_{\alpha^2 \to 0} X_1(\phi, \alpha^2, k) = C_2(\phi, k)$. The anisotropic part is obtained by direct substitution of $\beta = 0$ in equation (B13).

APPENDIX C

THE DENSITY OF STATES

Formula (4.157b) of BT87, after normalization of radii and energy to the core radius and central potential of the reference component, can be written as

$$\tilde{G}(\tilde{\mathscr{E}}) = \int_0^{s_M(\tilde{\mathscr{E}})} s^2 \sqrt{\tilde{\Psi}_T(s) - \tilde{\mathscr{E}}}\, ds , \tag{C1}$$

with $\tilde{\Psi}_T(s_M) = \tilde{\mathscr{E}}$. Changing the variable of integration from the radius s to the relative potential of the reference component, the result is

$$\tilde{G}(q) = \int_q^1 \sqrt{\tilde{\Psi}_T(\tilde{\Psi}) - \tilde{\Psi}_T(q)}\, \frac{(1 - \tilde{\Psi})^2}{\tilde{\Psi}^4}\, d\tilde{\Psi} , \tag{C2}$$

where the relation between q and $\tilde{\mathscr{E}}$ is given by equation (17). Again, as for the DF, it is convenient to discuss separately the two cases $\beta > 1$ and $0 \le \beta < 1$.

C1. THE CASE $\beta > 1$

Changing the variable of integration as in equation (B4), from equation (C2),

$$\tilde{G}^+(l) = 2b^{1/2} \int_l^{\sqrt{\beta}} \frac{\mathscr{G}(t) dt}{\sqrt{(\delta^2 + t^2)(t^2 - l^2)}} , \tag{C3}$$

where

$$\mathscr{G}(t) = 1 + \frac{2\beta - 4 + l^2 - \delta^2}{1 - t^2} + \frac{(\delta^2 - l^2)(3 - 2\beta) + \beta(\beta - 6) + 6 - \mu}{(1 - t^2)^2} + \frac{(1 - \beta)[(\beta - 3)(\delta^2 - l^2) + 2(\beta + \mu - 2)]}{(1 - t^2)^3} + \frac{(1 - l^2)(1 - \beta)^2(1 + \delta^2)}{(1 - t^2)^4} . \tag{C4}$$

After integration,

$$\frac{\tilde{G}^+(l)}{2b^{1/2} g} = X_0 + \frac{2\beta - 4 + l^2 - \delta^2}{1 - l^2} X_1 + \frac{(\delta^2 - l^2)(3 - 2\beta) + \beta(\beta - 6) + 6 - \mu}{(1 - l^2)^2} X_2 + \frac{(1 - \beta)[(\beta - 3)(\delta^2 - l^2) + 2(\beta + \mu - 2)]}{(1 - l^2)^3} X_3 + \frac{(1 - \beta)^2(1 + \delta^2)}{(1 - l^2)^3} X_4 , \tag{C5}$$

where the functions X_m are given in Appendix D, and their arguments are

$$g = \frac{1}{\sqrt{\delta^2 + l^2}} , \qquad k^2 = \frac{\delta^2}{\delta^2 + l^2} , \qquad \phi = \arccos\left(\frac{l}{\sqrt{\beta}}\right) , \qquad \alpha^2 = \frac{1}{1 - l^2} . \tag{C6}$$

C2. THE CASE $0 \le \beta < 1$

In this case,

$$\tilde{G}^-(l) = -2|b|^{1/2} \int_{\sqrt{\beta}}^l \frac{\mathscr{G}(t) dt}{\sqrt{(\delta^2 + t^2)(l^2 - t^2)}} , \tag{C7}$$

© American Astronomical Society • Provided by the NASA Astrophysics Data System

where $\mathscr{G}(t)$ is given in equation (C4). After integration,

$$\frac{\tilde{G}^{-}(l)}{-2|b|^{1/2}g} = V_0 + \frac{2\beta - 4 + l^2 - \delta^2}{1 - l^2} V_1 + \frac{(\delta^2 - l^2)(3 - 2\beta) + \beta(\beta - 6) + 6 - \mu}{(1 - l^2)^2} V_2$$
$$+ \frac{(1 - \beta)[(\beta - 3)(\delta^2 - l^2) + 2(\beta + \mu - 2)]}{(1 - l^2)^3} V_3 + \frac{(1 - \beta)^2(1 + \delta^2)}{(1 - l^2)^3} V_4 , \tag{C8}$$

where the functions V_m are given in Appendix D, and their arguments are

$$g = \frac{1}{\sqrt{\delta^2 + l^2}}, \qquad k^2 = \frac{l^2}{\delta^2 + l^2}, \qquad \phi = \arccos\left(\frac{\sqrt{\beta}}{l}\right), \qquad \alpha^2 = \frac{l^2}{l^2 - 1}. \tag{C9}$$

The case of the central BH is obtained from the previous two equations with the substitution $\beta = 0$.

APPENDIX D

ELLIPTIC AND JACOBIAN FUNCTIONS

Here I shortly summarize the notation for the special functions used, and their mutual relations, following BF71. The zeroth-order functions are

$$C_0(\phi, k) = D_0(\phi, k) = V_0(\phi, k) = F(\phi, k) . \tag{D1}$$

The mth-order functions are given by

$$C_2(\phi, k) = \frac{E(\phi, k) - (1 - k^2)C_0}{k^2}, \tag{D2}$$

$$C_{2m+2}(\phi, k) = \frac{2m(2k^2 - 1)C_{2m} + (2m - 1)(1 - k^2)C_{2m-2} + \mathrm{sn}\,(u)\,\mathrm{dn}\,(u)\,\mathrm{cn}^{2m-1}\,(u)}{(2m + 1)k^2} \tag{D3}$$

(BF71, eqs. [213.06]–[312.05]);

$$V_1(\phi, \alpha^2, k) = \Pi(\phi, \alpha^2, k) , \tag{D4}$$

$$V_2(\phi, \alpha^2, k) = \frac{\alpha^2 E(\phi, k) + (k^2 - \alpha^2)V_0 + (2\alpha^2 k^2 + 2\alpha^2 - \alpha^4 - 3k^2)V_1}{2(\alpha^2 - 1)(k^2 - \alpha^2)} - \frac{\alpha^4\,\mathrm{sn}\,(u)\,\mathrm{cn}\,(u)\,\mathrm{dn}\,(u)}{2(\alpha^2 - 1)(k^2 - \alpha^2)[1 - \alpha^2\,\mathrm{sn}^2\,(u)]}, \tag{D5}$$

$$V_{m+3}(\phi, \alpha^2, k) = \frac{(2m + 1)k^2 V_m + 2(m + 1)(\alpha^2 k^2 + \alpha^2 - 3k^2)V_{m+1}}{2(m + 2)(1 - \alpha^2)(k^2 - \alpha^2)} + \frac{(2m + 3)(\alpha^4 - 2\alpha^2 k^2 - 2\alpha^2 + 3k^2)V_{m+2}}{2(m + 2)(1 - \alpha^2)(k^2 - \alpha^2)}$$
$$+ \frac{\alpha^4\,\mathrm{sn}\,(u)\,\mathrm{cn}\,(u)\,\mathrm{dn}\,(u)}{2(m + 2)(1 - \alpha^2)(k^2 - \alpha^2)[1 - \alpha^2\,\mathrm{sn}^2\,(u)]^{m+2}} \tag{D6}$$

(BF71, eqs. [213.11]–[336.03]);

$$D_2(\phi, k) = \frac{(1 - k^2)D_0 - E(\phi, k) + \mathrm{tn}\,(u)\,\mathrm{dn}\,(u)}{1 - k^2}, \tag{D7}$$

$$D_{2m+2}(\phi, k) = \frac{2m(1 - 2k^2)D_{2m} + (2m - 1)k^2 D_{2m-2} + \mathrm{tn}\,(u)\,\mathrm{dn}\,(u)\,\mathrm{nc}^{2m}\,(u)}{(2m + 1)(1 - k^2)} \tag{D8}$$

(BF71, eqs. [211.09]–[338.05]);

$$X_m(\phi, \alpha^2, k) = \frac{1}{\alpha^{2m}} \sum_{j=0}^{m} (\alpha^2 - 1)^j \frac{m!}{j!(m - j)!} V_j \tag{D9}$$

(BF71, eqs. [211.14]–[338.04]).

In the previous expressions, the elliptic integrals of the first, second, and third kind are expressed as functions of the phase ϕ and the modulus k:

$$F(\phi, k) = \int_0^{\phi} \frac{d\theta}{\sqrt{1 - k^2\,\sin^2\,\theta}}, \qquad E(\phi, k) = \int_0^{\phi} \sqrt{1 - k^2\,\sin^2\,\theta}\,d\theta , \tag{D10}$$

$$\Pi(\phi, \alpha^2, k) = \int_0^{\phi} \frac{d\theta}{(1 - \alpha^2\,\sin^2\,\theta)\sqrt{1 - k^2\,\sin^2\,\theta}} . \tag{D11}$$

© American Astronomical Society • Provided by the NASA Astrophysics Data System

The relation of the elliptic integrals with the Jacobian functions for given (ϕ, k) are

$$u = F(\phi, k); \quad \text{cn}(u) = \cos\phi; \quad \text{sn}(u) = \sin\phi; \quad \text{dn}(u) = \sqrt{1 - k^2 \,\text{sn}^2(u)}, \tag{D12}$$

$$\text{tn}(u) = \frac{\text{sn}(u)}{\text{cn}(u)}; \quad \text{nc}(u) = \frac{1}{\text{cn}(u)}. \tag{D13}$$

REFERENCES

Bertin, G., Saglia, R. P., & Stiavelli, M. 1992, ApJ, 384, 423
Bertin, G., & Stiavelli, M. 1984, A&A, 137, 26
Binney, J. 1981, MNRAS, 196, 455
Binney, J., & Tremaine, S. 1987, Galactic Dynamics (Princeton: Princeton Univ. Press), chap. 4 (BT87)
Byrd, P. F., & Friedman, M. D. 1971, Handbook of Elliptic Integrals for Engineers and Scientists (2d rev. ed.; Berlin: Springer) (BF71)
Byun, Y.-I., et al. 1996, AJ, 111, 1889
Carollo, C. M. 1993, Ph.D. thesis, Ludwig-Maximilians-Univ., Munich
Carollo, C. M., de Zeeuw, P. T., & van der Marel, R. P. 1995, MNRAS, 276, 1131
Ciotti, L. 1991, A&A, 249, 99
Ciotti, L., & Lanzoni, B. 1996, A&A, submitted
Ciotti, L., Lanzoni, B., & Renzini, A. 1996, MNRAS, in press
Ciotti, L., & Pellegrini, S. 1992, MNRAS, 255, 561 (CP92)
Crane, P., et al. 1993, AJ, 106, 1371
Cuddeford, P., & Louis, P. 1995, MNRAS, 275, 1017
Dehnen, W. 1993, MNRAS, 265, 250
Dejonghe, H. 1986, Phys. Rep., 133, 217
de Vaucouleurs, G. 1948, Ann. d'Astrophys., 11, 247
de Zeeuw, P. T. 1996, in Gravitational Dynamics, Proc. 36th Herstmonceux Conf., ed. O. Lahav, E. Terlevich, & R. Terlevich (New York: Cambridge Univ. Press), in press
Dubinski, J., & Carlberg, R. G. 1991, ApJ, 378, 496
Eddington, A. S. 1916, MNRAS, 76, 572
Erdély, A., Magnus, W., Oberhettinger, F., & Tricomi, F. G. 1953, Higher Transcendental Functions (3 vols.; New York: McGraw-Hill)
Evans, N. 1993, MNRAS, 260, 191
Ferrarese, L., van den Bosch, F. C., Ford, H. C., Jaffe, W., & O'Connell, R. W. 1994, AJ, 108, 1598
Fridman, A. M., & Poliachenko, V. L. 1984, Physics of Gravitating Systems (2 vols.; New York: Springer)
Hernquist, L. 1990, ApJ, 536, 359 (H90)
Hunter, C. 1975, AJ, 80, 783
Hunter, C., & Qian, E. 1993, MNRAS, 262, 401
Jaffe, W. 1983, MNRAS, 202, 995
Jaffe, W., Ford, H. C., O'Connell, R. W., van den Bosch, F. C., & Ferrarese, L. 1994, AJ, 108, 1567
King, I. 1972, ApJ, 174, L123
Kormendy, J., et al. 1996, in IAU Symp. 171, New Light on Galaxy Evolution, ed. R. Bender & R. L. Davies (Dordrecht: Kluwer), 105
Lauer, T. R., et al. 1995, AJ, 110, 2622
Lynden-Bell, D. 1962, MNRAS, 123, 447
Merritt, D. 1985, AJ, 90, 1027
Møller, P., Stiavelli, M., & Zeilinger, W. W. 1995, MNRAS, 276, 979
Osipkov, L. P. 1979, AZh Pis'ma, 5, 77
Plummer, H. C. 1911, MNRAS, 71, 460
Sersic, J. L. 1968, Atlas de Galaxias Australes (Cordoba, Argentina: Obs. Astron., Univ. Nac. de Cordoba)
Stiavelli, M., & Sparke, L. S. 1991, ApJ, 382, 466
Tremaine, S. D., Richstone, D. O., Byun, Y.-I., Dressler, A., Faber, S. M., Grillmair, C., Kormendy, J., & Lauer, T. R. 1994, AJ, 107, 634
White, S. D. M. 1996, in Gravitational Dynamics, Proc. 36th Herstmonceux Conf., ed. O. Lahav, E. Terlevich, & R. Terlevich (New York: Cambridge Univ. Press), in press

© American Astronomical Society • Provided by the NASA Astrophysics Data System